Aerosol activation in marine stratocumulus clouds: 1. Measurement validation for a closure study

Sarah Guibert

Centre National de Recherche Météorologique (CNRM), Groupe de Météorologie Expérimentale et Instrumentale (GMEI/D), Météo-France, Toulouse, France

Jefferson R. Snider

Department of Atmospheric Science, University of Wyoming, Laramie, Wyoming, USA

Jean-Louis Brenguier

Centre National de Recherche Météorologique (CNRM), Groupe de Météorologie Expérimentale et Instrumentale (GMEI/D), Météo-France, Toulouse, France

Received 20 June 2002; revised 3 November 2002; accepted 27 January 2003; published 8 August 2003.

[1] This paper is the first of a series dedicated to an observational study of the aerosol indirect effect in marine stratocumulus clouds. The data were collected in 1997, during the second Aerosol Characterization Experiment (ACE-2) CLOUDYCOLUMN experiment, conducted over the eastern Atlantic Ocean, in the vicinity of the Canary Islands. Here we compare measurements made both on aircraft and at the surface, including condensation nuclei (CN) and accumulation mode aerosol concentrations, and aerosol size spectra. We also compare measured and predicted wet aerosol size spectra and examine statistics of vertical velocity within and below stratocumulus clouds. In general, aircraft and surface measurements of CN concentration, accumulation mode aerosol concentration and size spectra agree within expected uncertainties. However, a substantial disparity is documented in the comparison of predicted and observed wet aerosol spectra. We attribute this to either bias in the wet aerosol measurements, made with an FSSP-300, or to error in the sizing of dry aerosol particles. The analysis of vertical velocity indicates that the first and third moments of the vertical velocity frequency distribution do not change substantially between below-cloud and in-cloud flight segments; however, an increase in the second moment of the distribution across cloud base is documented. Overall, the results lend confidence to the use of surface site aerosol physical and chemical property data, as well as airborne measurements of vertical velocity, for modeling of the aerosol activation process, as described by *Snider et al.* [2003] (hereinafter referred to as part 2) in the special section. Here, and in the paper by *Snider et al.* [2003] (hereinafter referred to as part 2), we examine how sensitive the predictions are to the common assumption that the aerosol particles are compact spheres. *INDEX TERMS:* 0305 Atmospheric Composition and Structure: Aerosols and particles (0345, 4801); 0320 Atmospheric Composition and Structure: Cloud physics and chemistry; 1610 Global Change: Atmosphere (0315, 0325); 3307 Meteorology and Atmospheric Dynamics: Boundary layer processes; 3354 Meteorology and Atmospheric Dynamics: Precipitation (1854); *KEYWORDS:* marine aerosols, aircraft measurements, CCN closure

Citation: Guibert, S., J. R. Snider, and J.-L. Brenguier, Aerosol activation in marine stratocumulus clouds: 1. Measurement validation for a closure study, *J. Geophys. Res.*, *108*(D15), 8628, doi:10.1029/2002JD002678, 2003.

1. Introduction

[2] This paper is the first of a series examining the indirect effect of aerosol on climate via their interaction with marine stratocumulus cloud systems. The aerosol indirect effect (AIE) refers to the impact of aerosol on the radiative properties of clouds. It involves interaction among various physical and chemical processes, particularly the chemical transformation of gaseous species to form aerosol, aerosol coagulation, the activation of cloud condensation nuclei (CCN) to form cloud droplets, droplet coalescence to form drizzle, the transport and mixing of cloud parcels by turbulent eddies, and the effect of cloud properties on radiative transfer. Central to the topic is the subset of the aerosol population that act as CCN. When anthropogenic aerosol is added to the natural aerosol background generally both the CCN and the cloud droplet number concentration (CDNC) increase. CDNC thus varies with the origin of the air mass, from approximately 30 cm^{-3}

0148-0227/03/2002JD002678$09.00

in pristine marine air, to more than 1000 cm^{-3} in polluted regions. Assuming constant cloud liquid water content and vertical velocity, droplet sizes are constrained to smaller values in polluted clouds when compared to unpolluted clouds. This modification of droplet size affects cloud properties, such as cloud albedo [*Twomey*, 1977] and drizzle formation efficiency [*Albrecht*, 1989]. The first three papers of this series examine the aerosol/CCN/CDNC interaction, and also its parameterization in general circulation models (GCM), while the following papers examine the resulting impact on cloud microphysical and cloud radiative properties.

[3] The data analyzed in this series were collected during the second Aerosol Characterization Experiment (ACE-2), conducted in the vicinity of the Canary Islands, Spain [*Raes et al.*, 2000]. Measurements were made at a surface site and on three instrumented aircraft: (1) the Center for Interdisciplinary Remotely Piloted Aircraft Studies Pelican, (2) the Research Meteorological Research Flight C-130, and (3) the Météo-France Merlin. Hereinafter these aircraft are referred to as the Pelican, C-130, and M-IV, respectively. This special section extends previous analyses of data collected during the CLOUDYCOLUMN component of ACE-2 [*Brenguier et al.*, 2000a, 2000b; *Pawlowska and Brenguier*, 2000; *Snider and Brenguier*, 2000]. The prior analyses focused on local values of the relevant cloud and aerosol properties. Here we extend those results by considering the AIE phenomenon at scales comparable to that resolved by global climate models ($\sim$100 km). Motivation for this larger perspective comes from interest in validating predictions of the AIE in GCM and also in improving existing parameterizations.

[4] From the perspective of the aerosol/cloud interaction crucial to the AIE, previous analyses of the ACE-2 data set showed the following:

[5] 1. CCN measurements made at low supersaturations (S = 0.1%), on the Pelican, show no substantial departure from CCN measurements made concurrently on the M-IV or the C-130 [*Chuang et al.*, 2000]. Chuang et al. also show that CCN concentrations predicted based on Köhler theory, initialized with the measured and inferred properties of the aerosol overestimate measured CCN concentrations. That overestimation is $\sim$200% for the Pelican data set.

[6] 2. Clear-air and cloud interstitial aerosol number concentration measurements obtained during the HILLCLOUD component of ACE-2 were used to predict CDNC and those predictions were consistent with measurements made with a droplet aerosol analyzer [*Martinsson et al.*, 2000]. Comparison of that data with parallel CDNC values, obtained from a droplet spectrometer (FSSP-100), reveals a substantial disparity at CDNC values larger than 1000 cm^{-3}.

[7] 3. Aerosol size spectra from the C-130 during the LAGRANGIAN component of ACE-2, and used to predict the CCN concentration via Köhler theory, overestimate the measured CCN spectra. This discrepancy is reconciled if aerosol water soluble fractions (a parameter in the theory) is forced to be a factor of 2 to 3 smaller than that derived from chemical analyses of the submicron aerosol [*Wood et al.* 2000; *Snider and Brenguier*, 2000].

[8] 4. Predicted values of CDNC, based on airborne measurements of CCN activation spectra and vertical velocity from the M-IV, are in reasonable agreement with CDNC measurements from the M-IV [*Snider and Brenguier*, 2000].

[9] With the exception of the HILLCLOUD result, these studies reveal a systematic discrepancy among predicted and observed CCN concentrations, and therefore an error in the prediction of CDNC. Further, all predictions overestimate the observations. This conclusion is consistent with several other attempts to link observed and predicted CCN [*Bigg*, 1986; *Quinn et al.* 1993; *Covert et al.*, 1998]. Here, and in part 2, we examine how sensitive the predictions are to the common assumption that the aerosol particles are compact spheres.

[10] Understanding the cause of the CCN and CDNC discrepancies is necessary for improving confidence in physical models of the CCN activation process [*Ghan et al.*, 1993]. Ultimately, the objective of this research is the development of descriptions of the atmospheric aerosol, and their processing, so that precursor emissions, combined with meteorological or climatological models, can be used to predict CDNC in modeled clouds. An alternate approach is the technique proposed by *Van Dingenen et al.* [2000]. This consists of parameterizing CDNC by way of empirical relationships between aerosol volume (or mass) and the concentration particles larger than a specified size. This is employed in several GCM, but it is expected to overpredict CDNC in situations where the aerosol exits as a mixture of hygroscopic and nonhygroscopic particles and it models CDNC independent of vertical velocity.

2. Methodology

[11] In this paper (hereinafter referred to as part 1) and in part 2 [*Snider et al.*, 2003] we focus on four distinct analysis steps (Figure 1). Step 1 (in part 1) examines the issue of consistency between aerosol concentration measurements on four measurement platforms. To address this we will compare both condensation nuclei (CN) and accumulation mode aerosol measurements made at the surface site and on the M-IV, the Pelican, and the C-130. This is necessary since part of the disparity we discuss in the previous section, and in part 2, may be attributable to inefficient particle transmission through the aerosol inlets used on the aircraft, or to an enhancement of ambient concentrations in the vicinity of the surface site. The latter could occur if local aerosol sources bias the surface site measurements relative to that observed by the aircraft. These comparisons will be between measurements at the coastal surface site (described below) and on aircraft when they were sampling within marine boundary layer upwind (north) of the surface site. Step 2 (in part 1) examines consistency between predicted and observed aerosol size distributions at ambient relative humidity (RH). This closure is based on measurements of wet aerosol made with a FSSP-300 flown on the M-IV, and utilizes Köhler theory for the transformation from a dry aerosol spectrum (measured at the surface site) to a humidified spectrum at ambient RH. Step 3 (in part 2) examines comparisons of predicted and observed CCN concentrations. This closure also utilizes Köhler theory but in a fundamentally different way from that considered in step 2. Step 3 focuses on the relationship between dry size and critical supersaturation, i.e., the value of RH where a particle is released from its equilibrium constraint and can

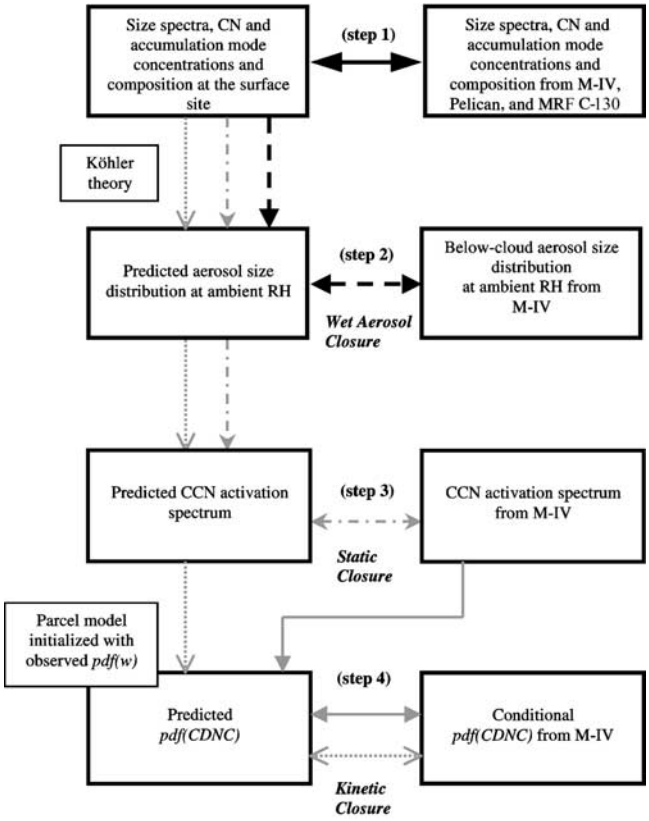

Figure 1. Methodology used for assessing the data set for consistency between multiple-platform measurements of aerosol size spectra, CN and accumulation mode aerosol concentration (step 1), for evaluating the wet aerosol closure (step 2), the static closure (step 3) and the kinetic closure (step 4).

therefore grow kinetically as a cloud droplet. The final closure (step 4, in part 2) utilizes a parcel model, a subcomponent of which is Köhler theory. It incorporates updraft values measurements, expressed as a probability distribution function, pdf (w), obtained from the M-IV. In anticipation of the need for pdf(w) in part 2, here we compare pdf(w) derived from M-IV sampling conducted both below cloud base and in-cloud. Note that throughout part 1 and part 2 we refer to steps 3 and 4 as the ''static'' and the ''kinetic'' closures, respectively.

[12] In summary, the objective in this first paper (part 1) is to examine the consistency of the CN, accumulation mode, and ambient wet aerosol measurements. We also examine airborne measurement of vertical velocity, and the variation of pdf(w) with height in the studied marine boundary layers. These results are then incorporated into the static and kinetic closure studies performed in part 2.

3. Instrumentation

3.1. Surface Instrumentation

[13] Surface measurements, made on the Punta del Hidalgo sampling tower, located on the northern coast of the Canary Island of Tenerife, include aerosol size spectra measurements conducted with a differential mobility analyzer (DMA), operated at a low relative humidity (20 ± 10% [*Putaud et al.*, 2000]), for particles in the 0.006 to 0.5 μm mobility equivalent size range, and with a TSI 33B Aerosol Particle Sizer (APS) for particles in the aerodynamic size range 0.5 to 29 μm (note that the counting efficiency of the APS is smaller than unity between 0.5 and 0.78 μm and that this issue is discussed further in section 7); CN concentrations derived by integrating the DMA size spectra (D > 0.01 μm); measurements of aerosol growth factor made with a Hygroscopic Tandem Differential Mobility Analyzer (HTDMA) [*Swietlicki et al.*, 2000]; and aerosol chemical composition measurements corresponding to dry particles smaller than ~0.85 μm [*Putaud et al.*, 2000]. The *Putaud et al.* [2000] data will hereinafter be referred to as measurements of submicron aerosol composition. Aerosol sampled by the DMA, APS and HTDMA systems were first drawn through an inlet that transmitted particles smaller than 15 μm.

[14] Implicit in our analysis of the size spectra are three assumptions. First, we assume that the particles were sized dry. This is consistent with the fact that air inside the inlet was heated by ~5°C relative to the ambient state, by the fact that the relative humidity (RH) of the DMA sheath air was 20 ± 10% [*Putaud et al.*, 2000], and by the fact that the temperature of aerosol entering the APS was increased by 10°C relative to that inside the inlet. We also assume that the mobility equivalent diameter, classified by the DMA, is equal to the sphere equivalent diameter. The latter is defined as the diameter that would result if the dried particle were compacted to form a sphere of density equal to 1700 kg/m^3. Errors introduced by this assumption are evaluated in section 7. Finally, for aerosol measured with the APS, the measured aerodynamic diameters (0.5 to 29 μm) were converted to sphere equivalent diameters (0.38 to 22 μm) on the assumption that the actual particles are spheres of density 1700 kg m^{-3}.

[15] With the exception of 7 July and the 3 days that we conducted short duration intercomparisons between the M-IV and the surface site (21 June; 4 and 19 July), the intercomparisons are based on flight interval averages. We have not shifted the averaging interval to account for the time required for air advection from the location of the aircraft to the surface site. Prior to averaging, the surface site measurements were screened to eliminate intervals that were not associated with onshore (northerly) flow. On 7 July we document a northeasterly aerosol property gradient and the averaging interval was therefore shortened (section 6.2).

3.2. M-IV Instrumentation

[16] The instrument payload flown on the M-IV during ACE-2 is described by *Brenguier et al.* [2000b]. We utilize humidity, temperature, vertical velocity, and aerosol and hydrometeor size spectra measured by the M-IV. These measurements, and their uncertainties, are discussed below.

[17] Three humidity probes were operated on the M-IV during ACE-2: a chilled-mirror dew point temperature sensor, a Lyman alpha absolute humidity sensor, and a capacitive RH sensor. The chilled-mirror instrument provides accurate values of the dew point temperature (±0.2 K) and was used as a reference for the two other probes. A disadvantage of the chilled-mirror sensor is its slow time

Table 1. Summary of the Surface Measurements and the Flights[a]

							Surface Site Measurements											
										Weight Percent Composition							
Date 1997	Origin	Air Mass	Flight Type	M-IV Track	Sub-Cloud Aircraft	PCASP	nss-SO_4 $\mu g/m^3$	NH_4/SO_4, Mole Ratio	ε, Soluble Fraction	OA	NO_3	nss-SO_4	NH_4	Sea Salt	OC	BC	Dust
21 June	NAM	INT	TEST	NW/SE	Pel	MIV/Pel	0.7	1.8	0.49	2	1	29	9	8	28	1	22
24 June	AT	MAR	TEST	N/S	NA	NA	0.2	2.0	0.67	3	4	30	11	19	32	0	1
25 June	AT	MAR	SCI*	SQ	NA	NA	0.2	1.9	0.75	3	4	32	11	25	25	0	0
26 June	AT	MAR	SCI*	SQ	C130	C130	0.3	2.0	0.48	2	2	21	8	15	25	0	27
04 July	PO	MAR	SCI	SQ	Pel	Pel	0.3	1.0	0.65	2	3	28	5	27	5	0	30
07 July	EU	POL	SCI	SW/NE	Pel	Pel	5.3	1.7	0.77	2	1	54	18	3	7	1	15
08 July	EU	POL	SCI*	SE/NW	NA	NA	4.6	1.8	0.91	2	1	64	20	4	8	1	0
09 July	EU	POL	SCI*	SQ	Pel	Pel	2.8	1.7	0.75	1	1	47	15	10	20	3	3
16 July	AT	INT	SCI*	SQ	C130/Pel	C130/Pel	1.5	1.7	0.81	2	1	57	17	4	16	3	1
17 July	EU	INT	SCI*	SQ	NA	MIV	1.6	1.7	0.63	1	1	45	14	2	27	8	2
18 July	EU	POL	SCI*	SQ	Pel	MIV/Pel	3.1	1.7	0.73	1	1	53	17	2	18	5	5
19 July	EU	INT	SCI*	SQ	C130/Pel	MIV/C130/Pel	1.4	1.1	0.89	2	1	60	13	13	9	1	1
21 July	EU	INT	TEST	N/S	NA	MIV	0.7	0.8	0.79	2	3	42	6	26	17	3	1
22 July	EU	NA	TEST	N/S	NA	MIV	NA	NA	NA	NA	NA	NA	NA	NA	NA	NA	NA

[a]The studied air masses are classified using back trajectories (at levels lower than 1 km mean sea level) and using submicrometric aerosol composition data from the surface site. The backtrajectories are summarized in the second column where the origin of the air arriving at the surface site is indicated (NAM, North America; AT, central Atlantic Ocean; PO, Polar; EU, European Union). Air masses are also classified based on submicrometric nss-SO_4 aerosol mass concentration measurements made at the surface site (MAR, maritime: nss-$SO_4 < 0.5$ $\mu g/m^3$; INT, intermediate: 0.5 $\mu g/m^3 <$ nss-$SO_4 < 2$ $\mu g/m^3$; POL, polluted: nss-$SO_4 > 2$ $\mu g/m^3$). Flight type indicates if the flight was a test flight or a scientific flight, and SCI* indicates flights for which *Pawlowska and Brenguier* [2000] report CDNC statistics. Aircraft are referred to as "Pel" for the CIRPAS Pelican, "C130" for the MRF C-130, and "MIV" for the Météo-France M-IV. The surface site measurements are described and analyzed by *Putaud et al.* [2000]. Relative uncertainties in soluble fraction are ±40%. NA, not available.

response (1/e response time ~20 s). Much faster response to ambient humidity variations was obtained from the two other probes but their absolute response to ambient humidity, for example within cloud, can depart by as much as 5% from the anticipated result (RH = 100%). These biases were minimized by employing a post-flight data correction procedure (private communication, B. Piguet, Météo-France). This involves finding flight segments corresponding to homogeneous below-cloud regions and then using humidity measurements from these regions to correct both the Lyman alpha and the capacitive humidity values so they agree with concurrent values derived from the chilled-mirror sensor. Our analysis of aerosol size as a function of RH utilizes data from the capacitive sensor, and on two flights, from the Lyman alpha sensor. The accuracy of the corrected RH values derived from those instruments is ± 3% between RH = 80% and RH = 100%.

[18] The air vertical velocity was measured on the M-IV with a differential pressure probe mounted on the nose radome. *Brown* [1993] conducted an error analysis of vertical velocity measurements made by a gust probe similar to that used on the M-IV. Random and systematic errors were estimated to be 0.1 m/s and 0.3 m/s, respectively. For the M-IV during ACE-2 the average vertical velocity, derived from sampling of horizontal below-cloud and in-cloud flight legs, was typically of magnitude less than 0.2 m/s, and never exceeded 0.4 m/s. Considering that the mean vertical velocity in the boundary layer is negligible, and that the measured average reflects an instrumental bias, this result is in agreement with the conclusions of *Brown* [1993]. The vertical velocity data set is analyzed in section 8 and there compared with prior observations, and to predictions based on large eddy simulations of a cloud-topped boundary layer.

[19] Data from aerosol and cloud microphysics probes mounted both externally and within the M-IV are used in this analysis. On the fuselage, three PMS probes measured the particle size distribution at ambient humidity: (1) the FSSP-300 [*Baumgardner et al.*, 1992] for the particle diameter range from 0.38 to 21μm, i.e., wet aerosol and droplets, (2) the Fast-FSSP [*Brenguier et al.*, 1998] for the range from 2.6 to 35 μm, i.e., cloud droplets, and (3) the OAP 200-X (PMS Inc., Boulder, Colorado, USA) for the range from 20 to 200 μm, i.e., drizzle drops. The FSSP-300 will be used to analyze below-cloud wet aerosol size spectra using bin boundaries corresponding to the refractive index of pure water. Since a larger refractive index is anticipated for the below-cloud aerosol this assumption should result in oversizing. This issue is discussed in section 7.

[20] Inside the M-IV three types of instruments measured the dried (RH < 50%) aerosol: (1) the UWyo CCN counter, operated at applied supersaturations that ranged between 0.2 and 1.6% [*Snider and Brenguier*, 2000], (2) a TSI 3760A CN instrument that detected particles of diameter larger than 0.01 μm, and (3) a Particle Measurement Systems (PMS) passive cavity aerosol spectrometer probe (PCASP) that measured accumulation mode particles in the diameter range from 0.1 to 3 μm [*Petzold et al.*, 1997]. Aerosol sample flow rates were either recorded and used in the data processing to calculate ambient concentrations (PCASP), or were held constant by a critical orifice placed between the instrument and the vacuum pump (TSI 3760A). These instruments sampled aerosol via two inlets. The CCN counter sampled via a quasi-isokinetic inlet that was located within a velocity diffuser. The upper cut-off diameter was estimated to be 8 μm [*Snider and Brenguier*, 2000], but that assessment only considers inertial effects and not particle loss via turbulent deposition. The estimated upper cut-off value is therefore an upper bound. The other aerosol instruments sampled via a reverse-flow inlet characterized by *Schröder and Ström* [1997], who estimated an upper cutoff diameter of 1 μm. Aerosol transmission by the reverse-flow inlet, compared to the quasi-isokinetic inlet, was tested

during two flights (21 and 22 July; see Table 1), while operating the M-IV several hundred meters above the stratocumulus cloud deck. The tests show that the CN concentration increases when switching from the reverse-flow to the quasi-isokinetic inlet. The increase was from 280 to 300 cm^{-3} and from 380 to 450 cm^{-3} on 21 July and 22 July, respectively. Larger relative increases, from 50 to 80 cm^{-3} and from 20 to 40 cm^{-3}, were documented for measurements made with the M-IV PCASP during the same tests. When this information is combined with our analysis of accumulation mode concentration measurements from the M-IV and other platforms (section 6.4), it suggests that the reverse-facing inlet did not transmit submicron particles as efficiently as expected from the work of Schröder and Ström.

3.3. C-130 and Pelican Instrumentation

[21] Both the C-130 and the Pelican usually flew the same pattern as the M-IV but at a lower altitude within the marine boundary layer. We analyze CN and accumulation mode aerosol data acquired by the C-130 during the three flights coordinated with the M-IV. The CN measurements were obtained from a TSI 3025 particle counter. The counting efficiency of this instrument is 50% at 0.003 μm diameter. The accumulation mode aerosol measurements were obtained using a PCASP mounted externally on the aircraft. Details of the C-130 ACE-2 data set are given by *Johnson et al.* [2000].

[22] During ACE-2 the Pelican flew four flights coordinated with the M-IV. Our emphasis is on the size spectra measured by the Pelican radial differential mobility analyzer (RDMA) and the Pelican PCASP. Like the C-130, the PCASP operated on the Pelican was mounted externally. Spectra obtained from both the RDMA and the PCASP were analyzed by *Collins et al.* [2000]. We utilize spectra derived from that analysis. These correspond to dried aerosol in the size range extending from 0.005 to 3 μm. The Pelican CN measurements we report were derived by integration of the combined RDMA/PCASP spectra ($D > 0.01$ μm).

4. Flights and Their Aerosol Chemical Context

[23] The fourteen M-IV flights conducted during ACE-2 are summarized in Table 1 and the flight patterns are illustrated in Figure 2. Ten of the flights were scientific flights and the other four were test flights. Seven of the scientific flights (25 and 26 June, 4, 9, 17, 18, and 19 July) were performed along a 60-km square flight-track. The square was positioned less than 300 km north of the Island of Tenerife. One additional scientific flight, also conducted along a 60 km square flight track, was positioned greater than 300 km northeast of the surface site (16 July). The remaining two scientific flights (7 July and 8 July) were performed along straight legs. The test flights (21 June, 24 June, 21 July and 22 July) were performed in the vicinity of Tenerife. With the exception of one of the test flights (21 July), all flights were conducted north and therefore upwind of the Canary Island chain. The M-IV was flown either at constant altitude (below cloud or in cloud) or along a saw-tooth trajectory that extended from below cloud base

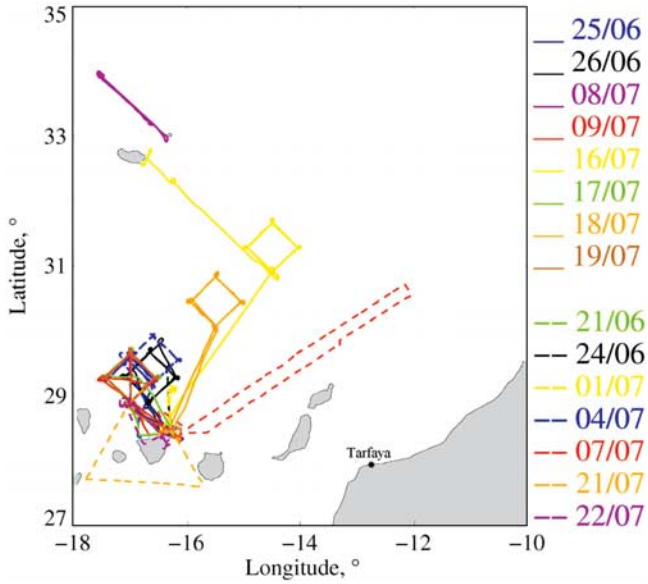

Figure 2. M-IV flight tracks during ACE-2.

to above cloud top. Constant-level legs, conducted below cloud base, were used for measuring aerosol, and CCN. Data acquired along the saw-tooth trajectories were used by *Pawlowska and Brenguier* [2000] to document vertical variations of CDNC and other cloud microphysical properties during eight scientific flights (indicated as SCI* in Table 1). Vertical velocity cannot be measured reliably during these ascending or descending flight sections. In this paper we therefore analyze vertical velocity data acquired along constant-level legs, made inside the cloud layer and below cloud base. That comparison is presented in section 8.

[24] Table 1 shows that either the Pelican or the C-130 participated in eight M-IV flights (21 and 26 June, 4, 7, 9, 16, 18, and 19 July). In general they flew a track similar to that of the M-IV but their positions were staggered. However, on 16 and 19 July both the C-130 and the Pelican participated to the CLOUDYCOLUMN mission (Table 1) and for safety reasons the Pelican flew a pattern that was displaced ~50 km from the tracks of the M-IV and C-130 [*Chuang et al.*, 2000].

[25] Submicron aerosol composition measurements made at the surface site during the M-IV flights indicate the range of air quality that was observed in the study region. These results (Table 1) when combined with trajectory calculations summarized by *Verver et al.* [2000] demonstrate that air trajectories originating from Europe are associated with polluted conditions while trajectories originating from the central Atlantic Ocean are much cleaner. Using non-sea salt sulfate concentrations as an indicator, we have classified the studied air masses as marine (nss-sulfate < 0.5 μg/m3, four flights), polluted (nss-sulfate > 2 μg/m3, four flights), and intermediate (0.5 μg/m3 < nss-sulfate < 2 ug/m3, five flights). A marine air mass, 26 June, and a polluted air mass, 9 July, are used in this paper to illustrate the differing aerosol properties associated with these two situations. The M-IV track on both of those days was a 60-km square positioned ~100 km north of Tenerife (Figure 2). Results obtained from our analysis of all flights are summarized in

tables and figures so that they can be used as input to future modeling exercises.

5. Aerosol Soluble Fraction

[26] For the closure studies involving wet aerosol (section 7) a key parameter is the aerosol water-soluble mass fraction ε. Using data from *Putaud et al.* [2000], and following *Snider and Brenguier* [2000], we define ε as the ratio of the submicron aerosol mass speciated as water-soluble ions (i.e., organic acid anions, sea salt, non-sea salt sulfate, ammonium and nitrate) divided by the total submicron aerosol mass. Note that we are assuming that the organic mass fraction, minus the relatively small mass contribution from the organic acid anions, is water insoluble and therefore nonhygroscopic. The derived values of ε are reported in Table 1 where we also present the submicron aerosol composition data used to calculate the soluble fraction. HTDMA measurements [*Swietlicki et al.*, 2000] demonstrate that the aerosol was internally mixed with regard to its hygroscopic properties. Further, the HTDMA growth spectra demonstrate that both Aitken and accumulation mode particles responded to increased humidification in a manner generally consistent with a uniform composition at all sizes (part 2). Table 1 also shows that the ammonium to sulfate mole ratio is nearly two, for most cases, and that a dominant mass category is obtained by combining ammonium and sulfate. Consistent with these results our Köhler theory calculations of wet size (section 7), corresponding to dry sizes smaller than 0.5 μm, are based on the assumption that the water soluble mass fraction is composed of ammonium sulfate. The value of the insoluble mass density was assumed equal to 1700 kg/m^3. Further support for these assumptions can be found in part 2 where we show that predicted hygroscopic growth factors agree with those measured to within 20%. With regard to the larger particles (dry size larger than 0.5 μm) we assumed they were composed of sodium chloride ($\varepsilon = 1$). Evidence in support of this assumption comes from the work of *Quinn et al.* [2000], who made ship-based measurements of size-resolved aerosol chemistry during ACE-2.

6. Aerosol Comparisons

[27] Here the properties of aerosol measured at the surface site are compared to those measured on the aircraft. The M-IV data used in this analysis are restricted to 1 Hz (about 90 m flight length) samples obtained from below-cloud regions containing no cloud droplets or drizzle drops, as both artificially increase the measured CN concentration via a process we refer to as liquid water shattering [*Snider and Brenguier*, 2000]. The cloud droplet criterion corresponded to the cumulative of the FSSP-300 spectrum between 3 and 21 μm (C_{300}). Similarly, the drizzle selection criterion was the cumulative of the OAP 200-X spectrum from 20 to 200 μm (C_{OAP}). Selection criteria used to define a sample not affected by liquid water shattering were $C_{300} < 2$ cm^{-3} and $C_{OAP} < 2$ cm^{-3}.

[28] Surface site aerosol measurements used in the comparisons are selected from time intervals corresponding to the flight intervals. In the comparisons the aerosol count is expressed as a number mixing ratio (i.e., aerosol number per unit mass of air) to account for the altitude difference between the surface site and the aircraft. The aerosol chemical composition measurements, discussed in section 6.1, are expressed as mass concentrations extrapolated to standard temperature (273 K) and pressure (1013 hPa).

6.1. Aerosol Chemical Composition Comparisons

[29] The surface site aerosol composition data set (Table 1) includes measurements of the dominant inorganic and organic ions, low solubility elements linked to terrestrial sources (e.g., Ca), and carbonaceous species. Using this data set, *Putaud et al.* [2000] performed a series of data quality and closure tests. They found that the chemically derived aerosol mass and the gravimetric aerosol mass agreed within ±40%. Further, and within comparable uncertainty limits, aerosol mass values inferred from composited DMA and APS size spectra also agreed with the chemically derived aerosol mass values. The mass closures obtained by Putaud et al. lend confidence to our estimates of the derived soluble fraction values but their work does not address the issue of vertical or horizontal gradients in aerosol chemical properties between the surface site and the location of the aircraft.

[30] By using aerosol composition measurements derived from filter samples collected on the C-130 (26 June and 19 July) when it was flying north of Tenerife, we examined the degree of consistency between the surface and airborne data. Because a limited suite of species was measured in samples collected on the C-130, compared to the surface site, the following discussion is limited to the species non-sea salt sulfate, sea salt, nitrate and ammonium. With one exception (non-sea salt sulfate on 19 July) C-130 concentrations exceeded those at the surface site. For sea salt and nitrate the discrepancy reflects the fact that the wet size cut used for sampling made on the C-130 (1.7 μm) was larger than that employed at the surface site (1.3 μm) and the fact that both nitrate and sea salt are enriched at supermicron sizes. Observations of nitrate and sea salt enrichment, during ACE-2, are presented by *Neusüß et al.* [2000] and *Quinn et al.* [2000], respectively. Ammonium concentrations were comparable on 26 June, both platforms reported 0.1 μg/m^3, while on 19 July the values reported by the C-130 were larger (0.6 versus 0.3 μg/m^3). However, in spite of the sampling bias resulting from the different size cuts, seven of the eight comparisons (again with the exception of non-sea salt sulfate on 19 July) were consistent within measurement uncertainty (±0.2 μg/m^3). For the 19 July non-sea salt sulfate comparison, the C-130 concentration (0.4 μg/m^3) was substantially smaller than that observed at the surface site (1.4 μg/m^3, Table 1). This result is consistent with the gradient detected in other aerosol property measurements on 19 July. This issue is discussed further in subsequent sections.

6.2. Condensation Nuclei Comparisons

[31] The first comparison of the CN data sets utilized data collected during M-IV flight segments flown within 500 m of the sea surface, and restricted to horizontal distances (M-IV to surface site) shorter than 30 km. Such data are available for the 4 July flight, conducted in a marine air mass, and for the 21 June and the 19 July flights, both

intermediate air masses. We refer to these flight segments as the fly-by comparisons. Excellent agreement is obtained for the 19 July case (440 mg^{-1}). During the two other flights the surface site mixing ratios were slightly lower than those of the M-IV, 510 versus 590 mg^{-1} on 4 July, 400 versus 480 mg^{-1} on 21 June. The results show that the surface and M-IV CN measurements agree within 20%, but with the M-IV CN measurement larger for two of the three comparisons. Because inlet tests indicated that a fraction of the aerosol is not efficiently sampled by the reverse-flow M-IV inlet (section 3.2), the actual disparity between CN measured at the surface site and on the M-IV may be approximately 10% larger than that indicated by these fly-by comparisons.

[32] For the second comparison of the CN data sets we consider aircraft CN measurements acquired at the location of the CLOUDYCOLUMN experiments, that is along M-IV flight tracks located farther away from the surface site than during the fly-by tests. Figures 3a and 3b show two such comparisons, expressed as CN frequency distributions, for 26 June (Figure 3a) and 9 July (Figure 3b). In both cases the surface site mixing ratios are slightly larger than the M-IV ones, but the 50th percentiles are in good agreement, 200 versus 226 mg^{-1} on 26 June, 608 versus 611 mg^{-1} on 9 July. Also note that the M-IV measurements show a few very high values (larger than 275 mg^{-1} on 26 June and larger than 650 mg^{-1} on 9 July) that are not observed at the surface site. These are possibly due to an incomplete rejection of aircraft measurements affected by liquid water shattering.

[33] Figure 4 summarizes comparisons of CN measurements from the three aircraft (M-IV, Pelican and C-130) versus that measured at the surface site. Each CN frequency distribution is represented by its mean value plus or minus one standard deviation. The flights analyzed by *Pawlowska and Brenguier* [2000] for CDNC characterization (SCI* in Table 1) are delineated by solid lines, and dashed lines are used to represent the other comparisons. The airborne measurements, acquired at 1 Hz, exhibit a larger variability than the surface values which were averaged over 10 min intervals. In general the agreement between aircraft and surface site concentration measurements stays within the 30% departure anticipated from the M-IV fly-by tests.

[34] Vertical profiles of M-IV CN measurements from 26 June, 9, 19 and 19 July are shown in Figure 5. Also plotted here are cloud base and top altitudes and also CN averages from the surface site, C-130 and Pelican, plus or minus their standard deviation. Recall that the M-IV performed several saw-toothed maneuvers through the cloud layer during each flight. Aircraft vertical speed during this maneuver was ~10 m/s and the profiles extended from ~200 m below cloud base to ~100 m above cloud top. For these flight segments the fraction of samples affected by liquid water shattering, and therefore the fraction rejected by the criteria discussed in section 6, is substantially larger than that for other flight segments. Note that some of the M-IV CN measurements made in the vicinity of the cloud layer, and plotted in Figure 5 because they passed the cloud droplet and drizzle drop sampling criteria (section 6), exceed that observed either above or below the cloud layer. This result is suggestive of samples that were not rejected but should have been. The case of July 16, which exhibits large CN mixing ratios in the free troposphere up to 1 km above the top of the cloud layer, is more difficult to interpret. For measurements made within the cloud layer on this day we cannot discriminate between a failure of the rejection procedure and valid CN measurements.

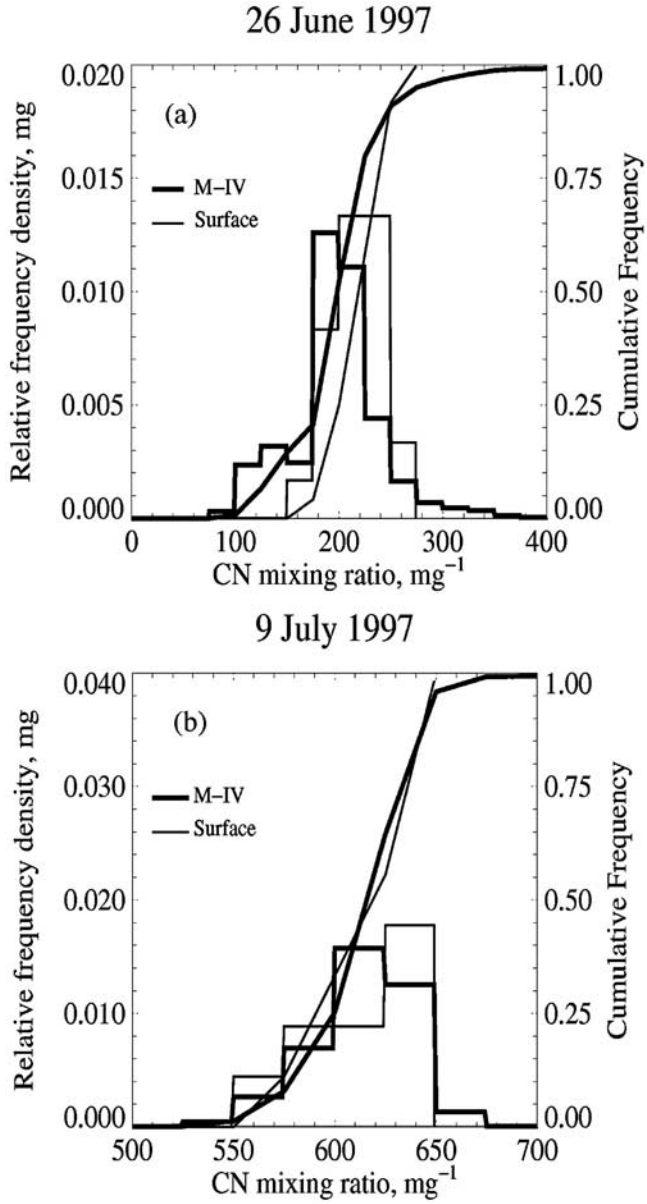

Figure 3. Frequency and cumulative distributions of the CN mixing ratio values measured on the M-IV (thick line) and at the surface site (thin line), on (a) 26 June and (b) 9 July.

[35] For the 26 June case (Figure 5a) the C-130 and surface CN data agree with the M-IV measurements. On 9 July (Figure 5b) the M-IV and the surface site measurements are less than 10% smaller than the Pelican. Another interesting aspect of the M-IV data set is apparent at altitudes above cloud top. Both cases (26 June and 9 July) exhibit a discontinuity at this interface. An analysis of the whole campaign reveals that the CN mixing ratio values in the free troposphere are relatively constant over the ACE-2 period

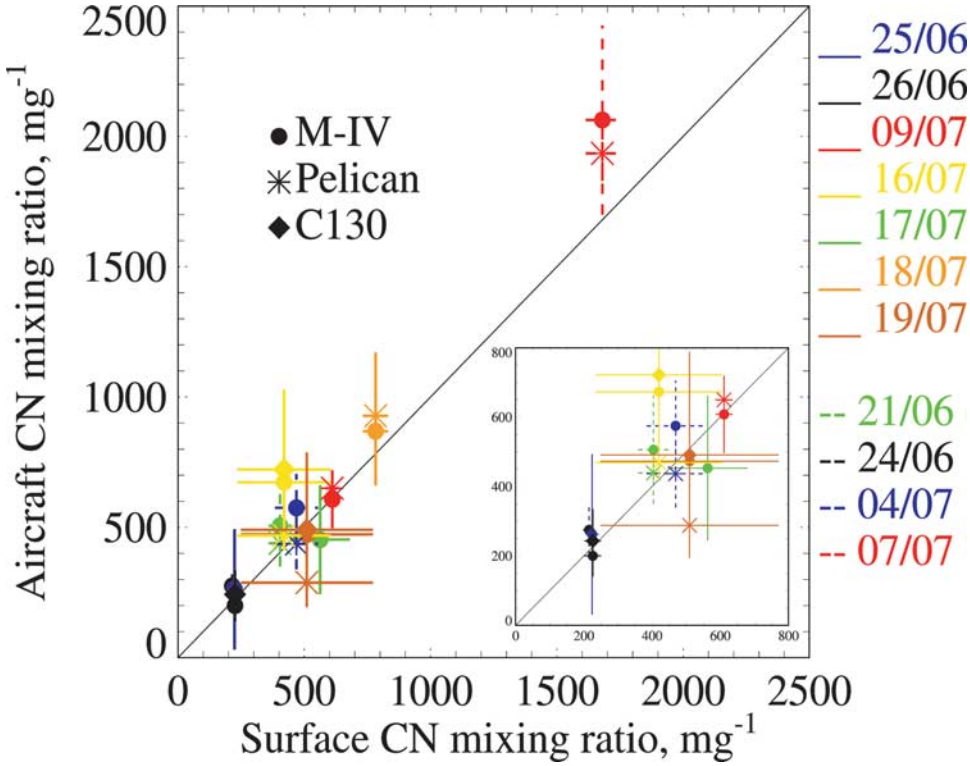

Figure 4. CN mixing ratio measurements performed on the M-IV (solid circles), the Pelican (stars) and the C-130 (solid diamonds), versus that measured at the surface site, with mean, plus or minus one standard deviation: Solid lines refer to M-IV flights analyzed by *Pawlowska and Brenguier* [2000] (SCI* in Table 1). Dashed lines refer to the other M-IV flights (SCI and TEST in Table 1).

($\sim$400 mg^{-1}), except for the 16 July, while the values measured in the boundary layer vary depending on the origin of the boundary layer air mass. These observations are in agreement with the results of *Verver et al.* [2000] showing that trajectories in the free troposphere are decoupled from those in the boundary layer.

[36] Figure 4 reveals that the 7 July case (M-IV and Pelican), and the 16 and 19 July cases (M-IV, Pelican and C-130), exhibit the poorest CN agreement. Here we examine if these inconsistencies can be explained by the existence of a spatially nonuniform marine boundary layer aerosol. CN averages, plotted as a function of horizontal distance for 7, 16, and 19 July are presented in Figure 6. A reference x-y position, and a horizontal direction aligned with the CN mixing ratio gradient, were picked for each case. For the 7 and 16 July cases the reference position was the surface site (28.30°N, 16.50°W, Figure 2), for 19 July the reference position was midway between the western and southern corners of the 60-km square (29.00°N, 17.50°W, Figure 2), and for all three flights the direction was northeastern (azimuth angle = 45°). Distances plotted in Figure 6 correspond to the component of the reference-to-aircraft vector aligned along the chosen horizontal direction. The plot was constructed using below-cloud CN values unaffected by liquid water shattering (section 6). Maximization of the absolute value of the slopes plotted in Figure 6 was the criterion used to define the reference position and the horizontal direction. Since no CN gradient was detected on 16 July the chosen reference position (28.30°N, 16.50°W) and direction (northeastward) are arbitrary.

[37] The 7 July CN values reported in Figure 4 were selected from boundary layer flight segments conducted no farther than 100 km from the surface site. The selected aircraft CN values were $\sim$20% larger than observed at the surface site (Figure 4). On this day Figure 6 demonstrates that the CN disparity can be attributed to a horizontal gradient directed from the surface site towards the African coast.

[38] On 16 July, Figure 4 shows that both the C-130 and the M-IV CN mixing ratio values are $\sim$55% larger than that observed either on the Pelican or at the surface site. Pelican data on this day are limited to the early part of the flight, at a distance of less than 30 km from the surface site, while the boundary layer C-130 and M-IV data correspond to flight segments executed 300 km to the north (Figure 2). The 16 July vertical profile data displayed in Figure 5c show that the free tropospheric CN mixing ratio values are much larger (up to 1500 mg^{-1}) compared to that observed in boundary layer. However, results shown in Figure 6 show no indication of a horizontal CN gradient in either the C-130 or the M-IV measurements, although boundary layer data from those aircraft is limited to positions 300 km north of the surface site. We speculate that the CN inconsistency (Figure 4) on 16 July is due to an unobserved horizontal CN gradient between the location sampled by the Pelican (30 km north of Tenerife) and the location of the 60 km square

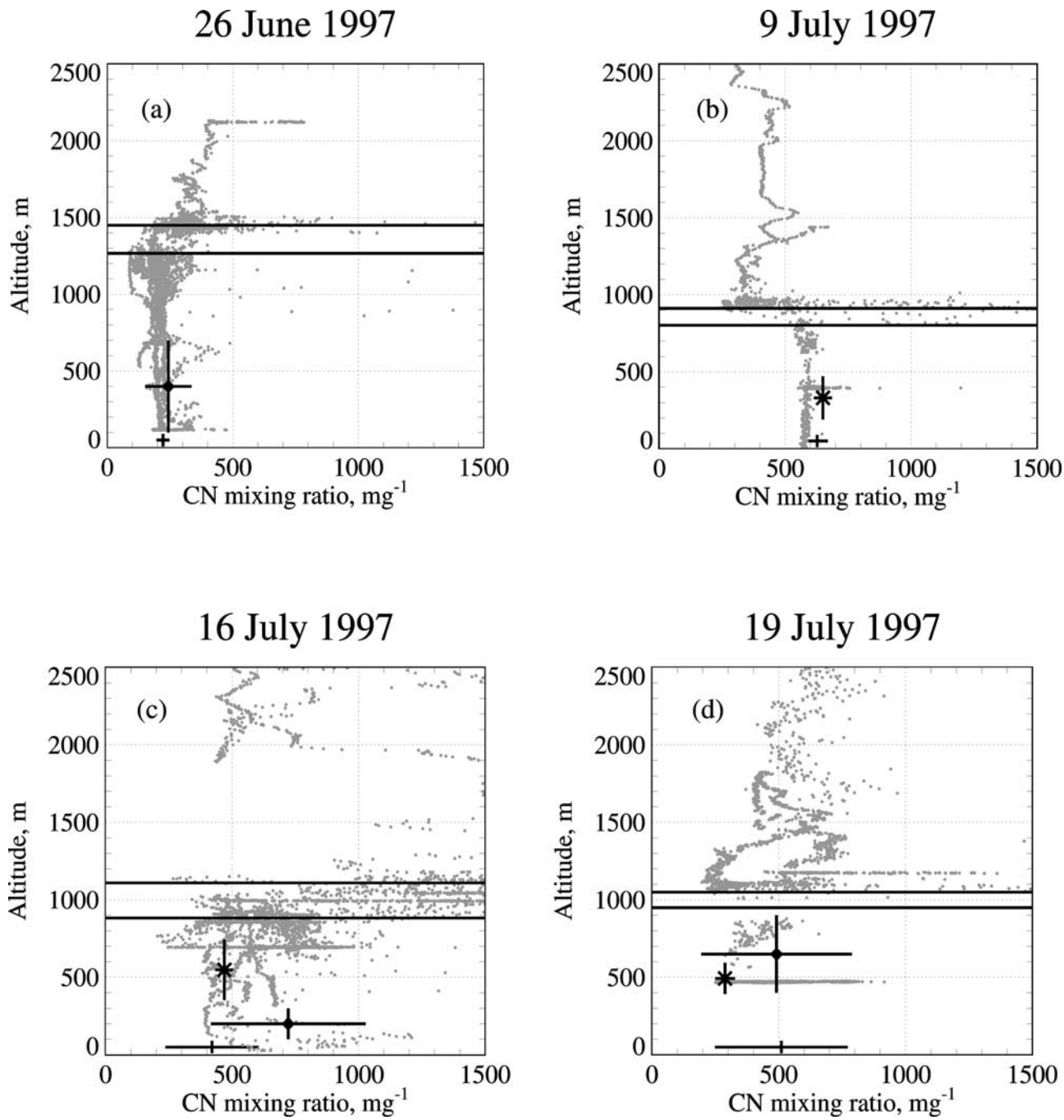

Figure 5. Scatterplots of M-IV CN mixing ratio versus altitude (indicated by gray dots). The surface site measurements are plotted at an altitude of 50 m. CN measurements from the Pelican (stars) and the C-130 (solid diamonds) are represented by their mean value, plus or minus one standard deviation and by a vertical segment showing their mean altitude, plus or minus one standard deviation. Airborne measurements are from (a) the C-130 on 26 June and (b) the Pelican on 9 July. Also indicated are the cloud base and cloud top altitude (black horizontal lines) for the four cases.

(~300 km farther to the north). Entrainment of CN from the free troposphere may have contributed to this gradient but there is insufficient data to support this contention.

[39] On 19 July the M-IV, C-130 and the surface CN measurements are consistent but values reported by the Pelican are 40% lower (Figure 4). Airborne CN measurements were confined to altitudes larger than 500 m on this day (Figure 5d). Above that altitude, but within the sub-cloud layer, the M-IV measurements vary between 300 and 800 mg^{-1}. The M-IV measurements (Figure 6c) reveal a southwesterly gradient, and hence the lowest CN values were observed by the Pelican which on this day was positioned northeast of the 60-km square shown in Figure 2 [*Chuang et al.*, 2000].

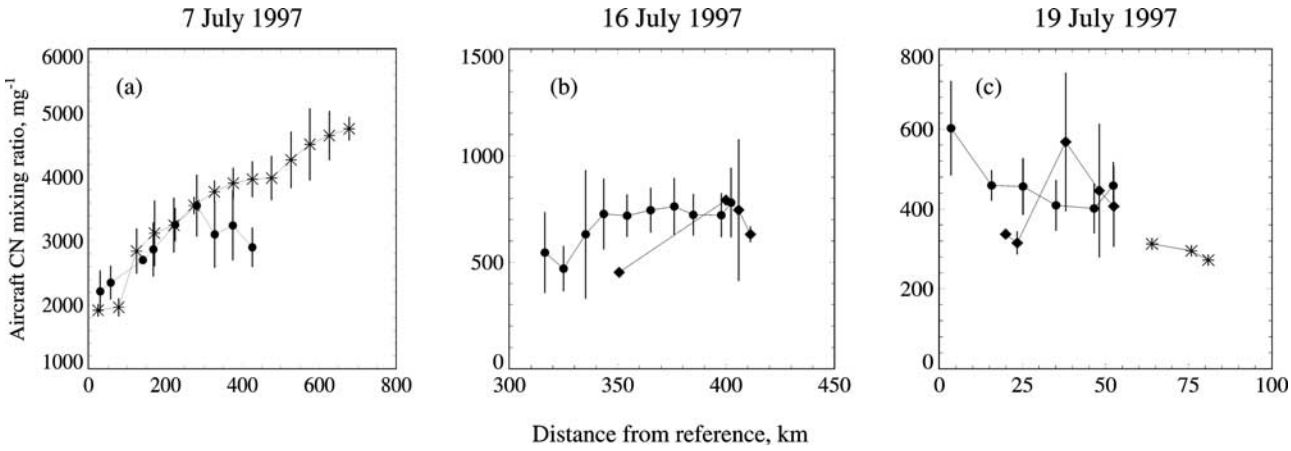

Figure 6. Horizontal variability of the CN mixing ratio measured on the M-IV (solid circles), on the Pelican (stars) and on the C-130 (solid diamonds). (a) M-IV and Pelican measurements on 7 July with the origin at the surface site. (b) M-IV and C-130 measurements on 16 July with the origin at the surface site. (c) M-IV, Pelican and C-130 measurements on 19 July with the distance measured from the south to west leg of the square M-IV track.

[40] Measurements discussed in the previous paragraphs indicate that marine boundary layer CN mixing ratios were spatially nonuniform on 7 and 19 July. This nonuniformity is apparent in Figure 6. On 16 July marine boundary layer CN measurements are not available for the region between the surface site and the 60-km square. CN vertical profiles obtained on 16 July do show a large mixing ratio increase between the marine boundary layer and the free troposphere (Figure 5c). We speculate that marine boundary layer mixing ratios were also spatially nonuniform on 16 July, and in particular between surface site and the 60-km square, but we note that the aircraft data cannot confirm this.

[41] The next section intercompares aerosol data obtained at sizes more relevant to the issue of CCN activation. We focus on dry particles in the 0.1 to 0.5 μm size range, and refer to them as accumulation mode aerosol.

6.3. Aerosol Size Spectra Comparisons

[42] Here, aerosol size spectra measured at the surface, with a DMA (section 3.1), are compared to measurements from the Pelican and the M-IV PCASP probes. Table 1, under the heading "PCASP," summarizes the flights for which the comparison is possible. During the test flight conducted on 21 June the PCASP from the C-130 was placed on the M-IV. This probe was mounted externally. For five other M-IV flights (17, 18, 19, 21, and 22 July) PCASP data were obtained from a probe mounted inside the M-IV (section 3.2). Accumulation mode size spectra from the Pelican were obtained by merging data from both the RDMA and the PCASP flown on the Pelican [*Collins et al.* 2000]. For these comparisons we assume that the measurements were made at relative humidities low enough to ignore size differences resulting from water associated with the sampled aerosol. Justification for that assumption is presented by *Snider and Brenguier* [2000] and by *Putaud et al.* [2000] for the M-IV and the surface site data, respectively. *Collins et al.* [2000] report that the measurements made on the Pelican were conducted at relative humidity values lower than ambient and also describe the technique used to infer the dried aerosol spectra from those actually measured. Their theoretically dried spectra are used in the following comparisons.

[43] Figures 7a and 7b show comparisons of surface site and Pelican spectra. Also indicated are Köhler theory predictions of the minimum dry diameter activated at 0.2, 0.4, 0.8 and 1.6% water vapor supersaturation, based on soluble fraction (Table 1) and our assumption that the soluble mass is ammonium sulfate (section 5). The averaged spectra and the average plus or minus one standard deviation (indicated by dashed lines and gray shading for the Pelican and surface site, respectively) are based on the numerous individual spectra measured during the 2–4 hour time intervals that the Pelican was flying north of the surface site and within the MBL. The overall consistency seen for 9 July (Figure 7a) is corroborated by the consistency shown by *Collins et al.* [2000] in their comparison of surface site, Pelican, and C-130 aerosol spectra measured during flights conducted on 14 July. Further, we found that measurements made with the C-130 PCASP, when operated externally on the M-IV on 21 July, are also consistent with the surface site data (not shown). Poorer agreement, but limited to Aitken mode sizes ($D < 0.1$ μm), is documented for 18 July (Figure 7b). Observe that lower spectral density values are reported by the Pelican at sizes between 0.08 and 0.15 μm. This discrepancy is obscured when integrating the size spectra for the comparison of the CN mixing ratios (Figure 4) or when integrating from 0.1 μm, to larger dry sizes, to compare accumulation mode mixing ratios, as is discussed in the following section. Parcel model simulations conducted by *Guibert* [2002] do exhibit some sensitivity to the 0.08 to 0.15 μm spectral density discrepancy. This results because the most vigorous vertical velocities observed on 18 July produce maximum supersaturations equal to 0.3% and thus activate particles with dry diameters larger than 0.08 μm.

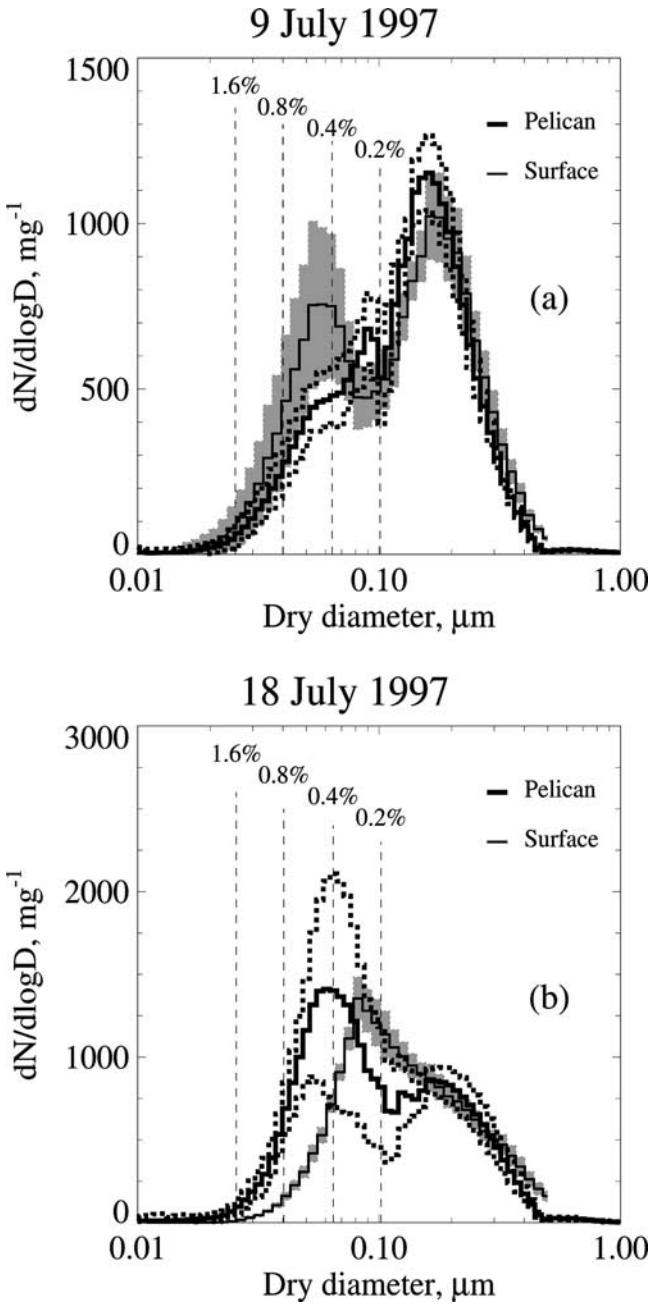

Figure 7. Dry aerosol size distributions on (a) 9 July and (b) 18 July, measured at the surface site (mean values indicated by the thin back line and the mean plus or minus one standard deviation by gray shading) and on the Pelican (mean values indicated by the thick black line and the mean plus or minus one standard deviation by the dashed black line. Vertical dashed lines indicate Köhler theory predictions of the minimum dry diameter activated at 0.2, 0.4, 0.8 and 1.6% water vapor supersaturation. The theory is based on the soluble fraction given in Table 1 and the assumption that ammonium sulfate is the water-soluble salt.

[44] Comparisons between surface spectra and those based on data from the PCASP operated within the cabin of the M-IV show that the latter underestimated the former. Those results are consistent with our findings of inefficient accumulation mode aerosol transmission through the reverse-flow inlet used to service the internally mounted M-IV (section 3.2).

6.4. Accumulation Mode Concentration Comparison

[45] Figure 8 summarizes the averaged mixing ratio values for the accumulation mode aerosol. The comparison was made by integrating the averaged size spectra from the lower diameter detected by the PCASP (0.1 μm) to the largest size detected by the surface site DMA (0.5 μm). With the exception of the 16, 17, 18 and 19 July cases, the M-IV, C-130 and Pelican data deviate by less than 30% from the surface measurements. On 16 and 19 July the discrepancy between the aircraft and the surface site is attributed to the spatial nonuniformity discussed in section 6.2. On 19 July the inefficiency of accumulation mode aerosol transmission into the M-IV PCASP (∼50%, section 3.2) obscures the fact that the location sampled by the M-IV had higher CN, and therefore presumably higher accumulation mode mixing ratio values, compared to the region sampled by the Pelican (Figure 4). Further evidence of the inefficiency of accumulation mode aerosol transmission into the internally mounted M-IV PCASP and also the smaller sampling bias introduced on M-IV CN measurements by the reverse-flow inlet, can be seen in the comparison of data collected on 17 and 18 July. Hence, in Figure 4 the 17 and 18 July CN measurements show good agreement among all platforms (M-IV and surface site on 17 July; M-IV, Pelican and surface site on 18 July) in contrast to undercounting by the internally mounted PCASP operated on the M-IV (Figure 8).

6.5. Summary of the Aerosol Comparisons

[46] In section 6.1 we examined a data set consisting of filter-pack measurements of aerosol chemical composition on 2 days (26 June and 19 July). These comparisons are not quantitative since different cut sizes were used for sampling (1.7 μm on the C-130 and 1.3 μm at the surface site). The data do confirm a result that is anticipated from size-resolved measurements of sea salt mass, i.e., that the mass distribution function dm/dlogD, increases geometrically with increasing size between ∼0.1 and ∼2 μm [*Quinn et al.*, 2000]. Hence for sea salt, and for nitrate which is also enriched at supermicrometric sizes [*Neusüß et al.*, 2000], our results (C-130 > surface site) were expected. The non-sea salt comparison based on 19 July data, the day with a southwesterly gradient in aerosol properties, did have significantly larger non-sea salt sulfate concentrations at the surface site.

[47] In sections 6.2, 6.3 and 6.4 we analyzed interplatform comparisons of CN and accumulation mode concentrations and comparisons of size spectra obtained from the aircraft and the surface site. We show that the M-IV CN measurements are comparable, within a relative uncertainty of 30%, to the measurements made at the surface site and on the Pelican and C-130. The accumulation mode mixing ratio values also agree within similar error limits. Two issues complicate this assessment. First, we have identified 3 days with spatially nonuniform aerosols. Nonuniformities are consistent with the larger CN mixing ratios detected by the M-IV and the C-130, relative to the surface site and the Pelican, on 16 July, the smaller CN mixing ratios detected by the Pelican, relative to the surface site and M-IV, on 19 July, and the larger CN mixing ratios detected by the M-IV and

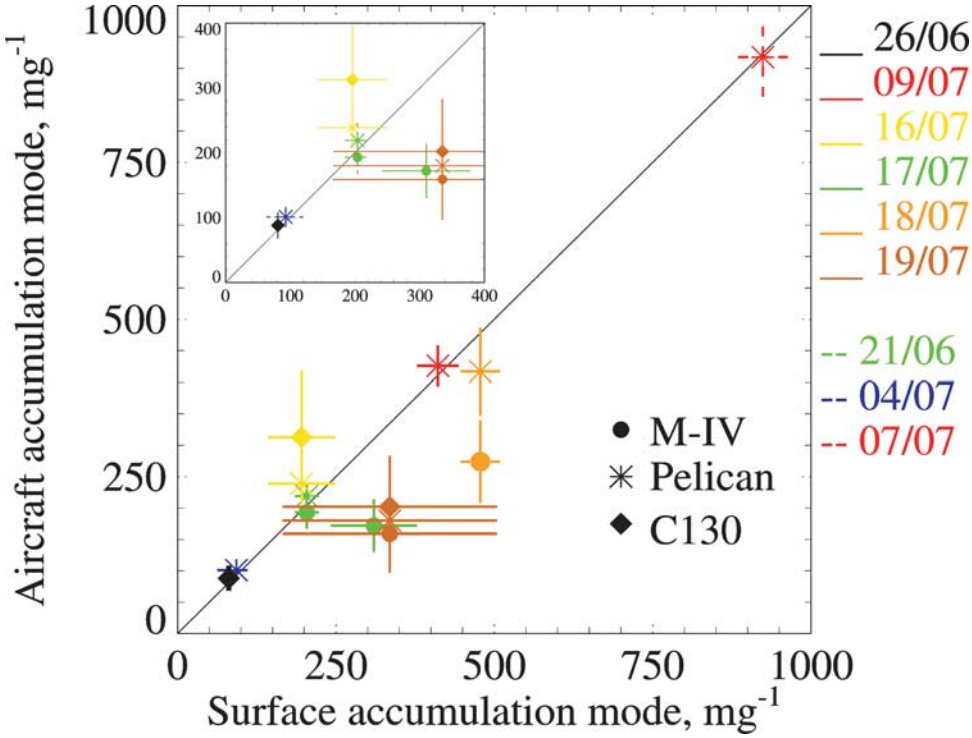

Figure 8. Accumulation mode aerosol mixing ratios, obtained by integrating size spectra from 0.10 to 0.50 μm. Comparison between airborne and surface site measurements. Symbols as in Figure 4.

the Pelican, relative to the surface site, for flight segments conducted close to the African coast on 7 July. Second, the inlet used on the M-IV for both the CN and the internally mounted PCASP did not efficiently transmit accumulation mode aerosol. Hence the comparisons shown in Figure 8 reveal a negative bias in the M-IV data collected on 17 July, 18 July and 19 July. With the exception of data from 16 July and 19 July, and the 7 July data collected near the African coast, and disregarding the accumulation mode measurements made on the M-IV with the internally mounted PCASP, our analysis indicates that the surface measurements are representative of aerosol properties in the area north of Tenerife at the altitude of the airborne measurements, at least for two aerosol physical properties (i.e., the CN and accumulation mode aerosol mixing ratios).

[48] Our analysis is inconclusive with regard to the consistency of airborne and surface site dry size spectra, particularly at Aitken mode sizes ($D < 0.1$ μm). Two flights, both exhibiting reasonable CN and accumulation mode consistency, are available for analysis (9 and 18 July). Results are shown in Figure 7. The comparison reveals a spectral density mismatch at Aitken mode sizes and that the mismatch is more pronounced on 18 July, particularly at dry sizes corresponding to the smallest particles expected to nucleate cloud droplets. *Guibert* [2002] evaluates the effect of this spectral density mismatch on CDNC and shows that it will result in a 15% overestimation if the Pelican spectrum is assumed to be correct.

7. Wet Closure

[49] The aerosol soluble fraction data (Table 1) and dry size spectra, measured with the surface site DMA and the APS, are used here to calculate wet size spectra for comparison with those measured directly with the FSSP-300. In the calculations, which are based on Köhler theory (part 2), we assume that the water soluble material at dry sizes smaller than 0.5 μm is ammonium sulfate, that these particles are internally mixed, and that particles larger than 0.5 μm are composed of sodium chloride (section 5). Further, superimposed bi-mode lognormal fits of the DMA ($D < 0.5$ μm) and the APS data ($D > 0.78$ μm) are used to define the aerosol spectra density at dry sizes larger than 0.5 μm. This is necessary since the APS counting efficiency is less than unity at dry spherical equivalent sizes smaller than 0.78 μm (E. Sweitlicki, private communication) and since a parameterized description of the largest aerosol particles is desired for the studies discussed in part 2. The inferred wet size spectra were calculated at 87, 92 and 97% RH. FSSP-300 size spectra were sampled with the following criteria: $87\% < RH < 97\%$, $C_{OAP} < 2$ cm^{-3} and $C_{300} < 2$ cm^{-3}. Recall that C_{300} is the concentration larger than 3 μm reported by the FSSP-300 (Section 6). Figure 9 shows the averaged FSSP-300 spectra, their variability and the predictions for 26 June (a) and 9 July (b). At sizes larger than 5 μm there is reasonable agreement between the observed and predicted wet spectra. When expressed as a comparison of predicted and observed particle mixing ratios, in the 5 to 21 μm wet size range, the agreement is within a factor of 2, and for most of the cases the agreement is within ±20%.

[50] Figure 10 shows the comparison of the particle mixing ratio in the DMA and FSSP-300 overlapping size range, i.e., by cumulating wet size spectra between 0.38 μm (detection threshold of the FSSP-300) and the wet diameter corresponding to a 0.5 μm dry particle (upper limit of the

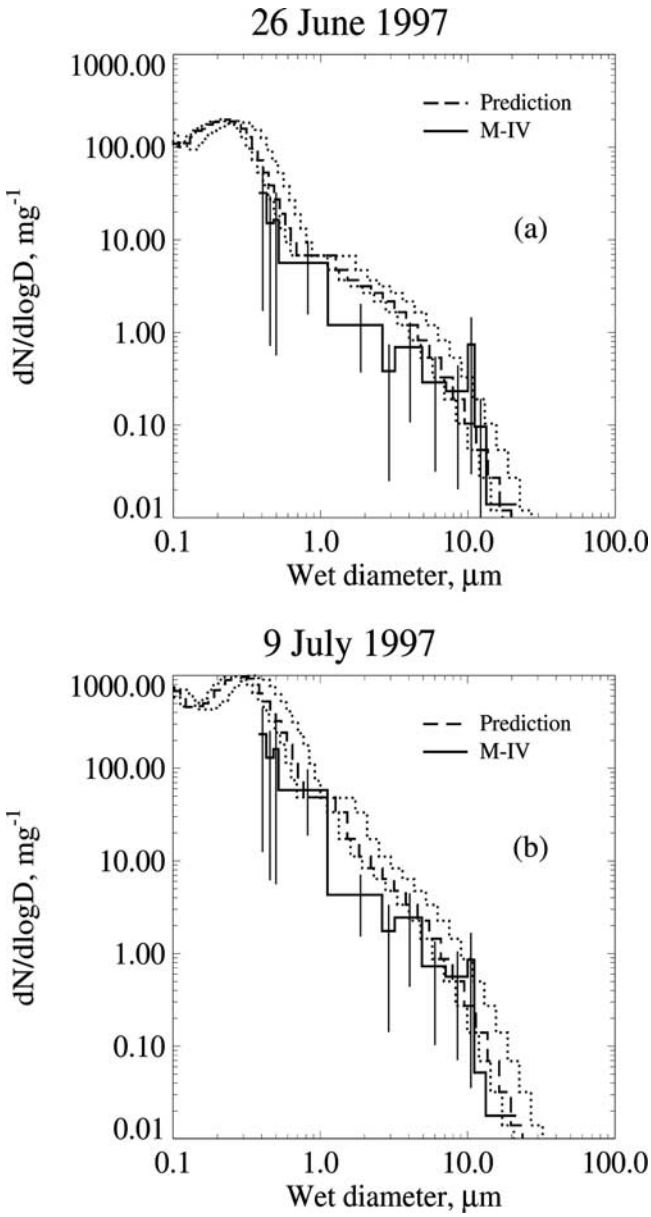

Figure 9. Wet aerosol size distributions on (a) 26 June and (b) 9 July, measured with the M-IV FSSP-300 (thick line is the average; short vertical lines indicate the average plus or minus 1 standard deviation in each diameter bin) compared to predicted wet size spectra based on surface size spectra measurements (dashed line is for the calculation performed at RH = 92%, dotted lines show the calculated result at RH = 87% and at RH = 97%).

DMA). The upper value (~0.8 μm) depends upon the soluble fraction. Mixing ratios corresponding to the predicted spectra exceed the FSSP-300 measurements. This discrepancy is a minimum on 26 June (marine air mass) and largest on 7 July (polluted air mass). Note that on both days the aircraft and surface measurements of the accumulation mode concentration (an integral from 0.1 to 0.5 μm, based on the dry size spectra) are in good agreement (Figure 8), and that this conclusion is also true for 21 June, 4 July, 9 July, and 18 July. (The outlying data points seen in Figure 8 are discussed in sections 6.5). Given the consistency of surface and airborne accumulation mode concentrations, and the consistency of surface and airborne accumulation mode size spectra (section 6.3), spatial nonuniformity of the aerosol is not a viable explanation for the systematic disparity seen in Figure 10. In the following paragraphs we discuss plausible causes for this disparity. First we focus on parameters input into the Köhler theory, second on the FSSP-300 spectra, and third on the sampling criteria.

[51] Smaller soluble mass fractions, substantially smaller than that anticipated after reducing the nominal values of ε by 40% (consistent with the ±40% relative error in submicron mass (section 6.1)), or aerosol hygroscopicities substantially smaller than that anticipated for ammonium sulfate, are two plausible adjustments that could force an acceptable wet aerosol closure. Since both of these adjustments contradict the submicron mass closure reported by *Putaud et al.* [2000], we will discuss a more plausible correction. DMA measurements of particle size are derived using a model which assumes that the particles are spheres. If in fact the particles are aspherical, or if the particles are porous, then the DMA model overestimates the sphere equivalent size. This overestimation can be expressed in terms of the sphere equivalent and the mobility equivalent diameters; the latter being the size derived from the electrical mobility measurement, via the DMA model, and the former is defined in section 3.1. Indeed, after assuming that the sphere equivalent by mobility equivalent diameter ratio is 0.8, the slope of the best-fit of FSSP-300 versus predicted wet aerosol mixing ratio values increases from 0.2 to 0.5, for the four marine cases, and increases from 0.2 to 0.3 for the four polluted cases. This sizing correction is at the extreme of that anticipated from laboratory characterization of submicron aerosols prepared by spray atomization [*Sioutas et al.*, 1999] (part 2). This result indicates that sphere equivalent to mobility equivalent diameter ratios smaller than that observed in the laboratory, or a hidden measurement bias, are needed to achieve an acceptable wet aerosol closure for this data set.

[52] Particle undersizing by the FSSP-300 could also explain the disparity documented in Figure 10; however, we used sizing thresholds corresponding to pure water which should cause oversizing since the actual solution droplets contain materials (sulfate and ammonium) which are known to enhance the refractive index. Thus FSSP-300 sizing thresholds consistent with a refractive index larger than that assumed would result in an even larger inconsistency that that shown in Figure 10. Another plausible explanation is that particle concentrations reported by the FSSP-300 were underestimated because of an error in the beam section used to process the FSSP-300 data; however this seems unlikely, at least to the extent needed to account for the disparity, since the beam section error is nominally ±15% [*Baumgardner et al.*, 1992].

[53] The observed lack of closure may also point to ambiguities associated with the selection of wet size spectra. To better understand the effect of the cloud droplet rejection criterion (section 6) on the sampled FSSP-300 spectrum, we omitted that particular criterion, resampled the sub-cloud data and recomputed the measured wet spectrum. At supermicron sizes a factor of 2, or smaller, increase of the averaged FSSP-300 spectral densities was

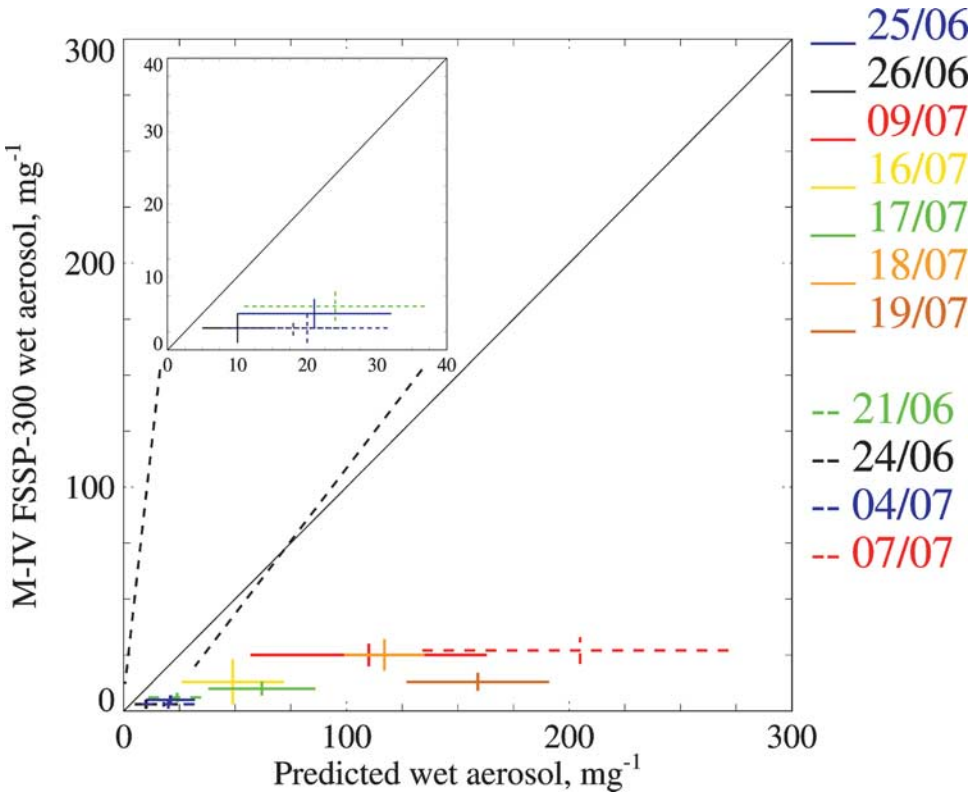

Figure 10. Particle mixing ratio cumulated in the range of wet diameter 0.38 to 0.80 μm, as measured with the M-IV FSSP-300 at ambient RH between 87 and 97%, versus predictions at RH equal to 87, 92, and 97%. Solid and dashed lines as in Figure 4.

observed, presumably due to the sampling of evaporating droplets, but the exercise did not substantially increase the FSSP-300 spectral densities in the 0.38 to 0.8 μm size range. This result, combined with the fact that some data segments associated with liquid water shattering were missed by the cloud droplet and drop rejection criteria (section 6.2), suggest that improvements in dry and wet aerosol size spectrometers, as well as increased efforts aimed at intercomparing these instruments in a controlled laboratory setting, are needed to advance understanding of ambient wet size spectra, particularly at wet sizes smaller than ~5 μm.

8. Vertical Velocity

[54] In an updraft CDNC is determined by the wet aerosol size distribution, by the chemical composition of the solution droplets, and by the kinematic history of the ascending air parcel. Using an aircraft to track air parcels, and thus to record their kinematic history, is not feasible. Lacking that information necessitates assumptions about the nature of vertical motion within a marine boundary layer, and air parcel trajectories during the CCN activation process. We assume that (1) the distribution of vertical velocities w within the boundary layer is characterized by an average of zero, and (2) that w does not vary substantially over the vertical displacement (10 to 50 m) required for production of the peak supersaturation at, or slightly above, the altitude of cloud base. Assumption (1) neglects any effect due to changes in the depth of the marine boundary layer, but the corresponding velocities, of order 0.001 m/s, are small in comparison to vertical speeds associated with boundary layer turbulence. These assumptions are the basis for the kinetic closure study conducted in part 2. Here we test the data used to conduct that study (i.e., the first assumption) and also examine the plausibility of our second assumption. These investigations utilize w statistics based on 10 Hz M-IV gust probe data collected both below cloud base and within the cloud layer. The sampling of w is restricted to those portions of the M-IV data that correspond to level and straight flight segments (section 3.2) [*Snider and Brenguier*, 2000].

[55] Vertical velocity frequency distributions from 26 June and 9 July are shown in Figures 11a and 11b. Thick solid lines correspond to data collected below cloud base and thin lines to data obtained within the cloud layer. Distribution averages are indicated on the x axis and a summary of results obtained from the whole campaign is presented in Tables 2a and 2b. The tabulated vertical velocity statistics are segregated by flight type. Results from the 5 days analyzed in part 2, four of which were conducted within 100 km of the surface site, are presented in Table 2a. These results are used in part 2 to perform model calculations of CDNC. Vertical velocity statistics from other flights are presented in Table 2b. With a few exceptions early in the campaign, averages are smaller than 0.3 m/s and thus smaller than the measurement bias anticipated by *Brown* [1993] (see section 3.2). This supports our assumption that the derived vertical velocity frequency distributions can be used to make reliable statistical predictions of CDNC in

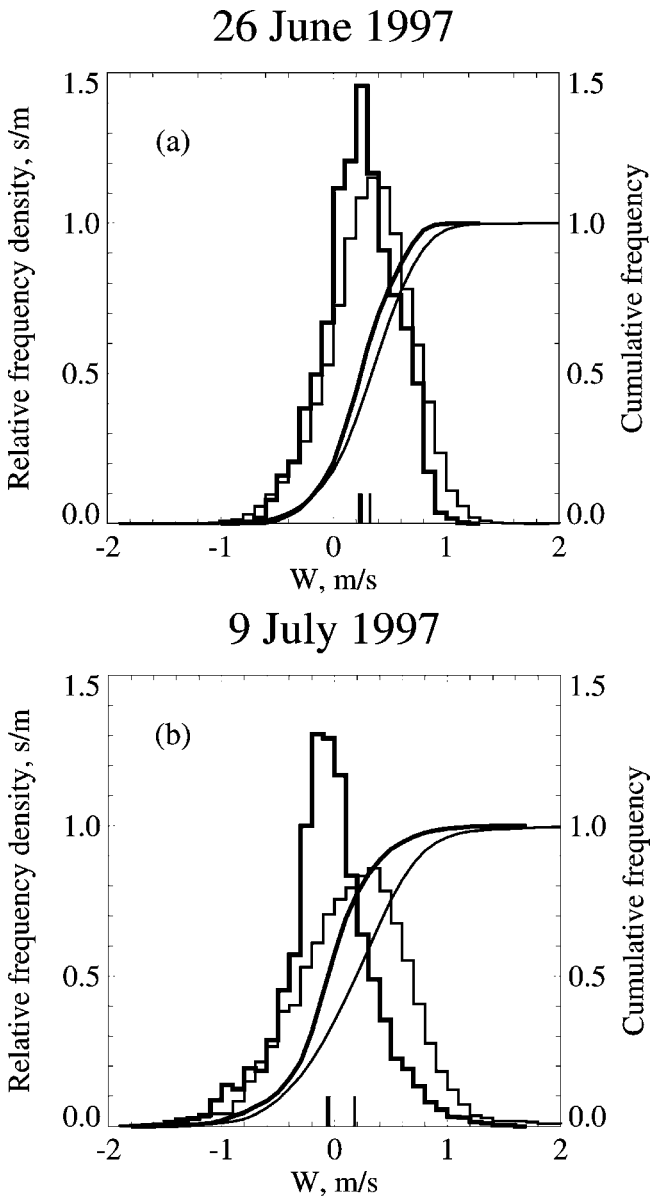

Figure 11. Frequency and cumulative distributions of measured vertical velocity on (a) 26 June and (b) 9 July; thick solid lines for data collected bellow cloud base and thin lines for data collected in cloud. The vertical bars on the *x* axis represent the mean values of the distributions.

part 2. Also supporting this is the fact that the standard deviations vary over a range that is consistent both with other observations of marine stratocumulus [*Boers et al.*, 1998] and with numerical studies of turbulence in a cloud-topped boundary layer [*VanZanten et al.*, 1999]. The results presented in Tables 2a and 2b also support our assumption of constant vertical velocity for individual parcels advecting across cloud base since they show no trend between the below-cloud and in-cloud averages, nor any trend in the height-stratified values of the skewness parameter. There is, however, evidence of a small increase in the vertical velocity standard deviation between the below-cloud and in-cloud flight legs.

[56] In addition there is an issue that arises from a characteristic of the vertical velocity pdf derived from aircraft. Airborne measurements of *w* are often interpreted as a space distribution, and specifically as that resulting from sampling from a fixed, or Eulerian, reference frame [*Panofsky and Dutton*, 1984]. In contrast, the vertical velocities we use in the parcel model of part 2 are assumed to come from a Lagrangian reference frame. Further, model simulations suggest that the Lagrangian mean vertical velocity, and not its fluctuations, is the primary determinant of the predicted CDNC [*Guibert*, 2002]. Since the gust-probe measurement of *w* (the Eulerian velocity) is the vector sum of Lagrangian mean vertical velocity and its local fluctuations, it follows that the vertical velocity standard deviations we report are enhanced relative to that which controls the actual standard deviation of the pdf of CDNC. Quantification of this enhancement will require a measurement strategy different from that employed here.

9. Conclusion

[57] We have tested the hypothesis that surface aerosol measurements, made on the north coast of the Canary island of Tenerife, can be extended to the marine boundary layer upwind of the island. The results indicate that for a majority of the cases the compared surface- and aircraft-based aerosol measurements agree within reasonable uncertainties. However, the comparison of the aerosol chemical composition measurements is incomplete because of differences in the size cuts used for sampling aerosol on the C-130 and at the surface site and also because of the few number of aircraft samples that were obtained during the CLOUDYCOLUMN experiments.

[58] We also analyzed vertical velocity frequency distributions derived from measurements made with the M-IV gust probe. These statistics are used as input to the CDNC closure study performed in part 2. Three observations are evident from the analysis: (1) Vertical velocity averages are generally smaller than the measurement bias anticipated by *Brown* [1993] and exhibit no tendency to be larger within the cloud compared to below it; (2) the vertical velocity skewness parameter is smaller than that observed in small cumulus [*Roode and Duynkerke*, 1996] and exhibits no tendency to be larger within the cloud compared to below it; and (3) standard deviations are slightly larger within the cloud layer, and the range of observed values is consistent with prior observations of marine stratocumulus and with simulations of turbulence within boundary layer clouds. Our observation that the vertical velocity standard deviation increases across cloud base limits the validity of the assumption that individual parcels advect across cloud base at a constant vertical velocity, but as we show in part 2, the resulting ambiguity is small relative to uncertainties associated with aerosol properties.

[59] Exceptions to the overall consistency consist of the following:

[60] 1. Surface and M-IV accumulation mode aerosol concentration comparisons reveal a bias (M-IV < the surface site). This is attributed to inefficient aerosol transmission into the internally mounted PCASP on the M-IV. Test flight data validate that assertion. It is also corroborated by concordance between measurement made with an exter-

Table 2a. Vertical Velocity Statistics for the Five Scientific Flights Analyzed in Part 2[a]

Date 1997	Flight Type	Cloud Base Altitude, m	Altitude of Sampling, m	Number of Data Points	Median Value, m/s	Average Value, m/s	Standard Deviation, m/s	Skewness
25 June	SCI*	1241	1420[b]	1301[b]	0.35[b]	0.33[b]	0.52[b]	−0.0[b]
			534[c]	5000[c]	0.15[c]	0.17[c]	0.39[c]	0.4[c]
26 June	SCI*	1267	1330 and 1400[b]	19750[b]	0.34[b]	0.32[b]	0.37[b]	−0.1[b]
			1158[c]	3000[c]	0.24[c]	0.24[c]	0.31[c]	−0.2[c]
9 July	SCI*	802	815 and 840[b]	8942[b]	0.19[b]	0.18[b]	0.50[b]	0.2[b]
			393[c]	6000[c]	−0.06[c]	−0.05[c]	0.41[c]	−0.1[c]
17 July	SCI*	918	1040 and 1070[b]	13222[b]	0.07[b]	0.03[b]	0.36[b]	−0.6[b]
			273[c]	6000[c]	0.04[c]	0.07[c]	0.28[c]	0.8[c]
18 July	SCI*	837	910 and 950[b]	7587[b]	0.10[b]	0.10[b]	0.55[b]	0.6[b]
			684[c]	6000[c]	0.21[c]	0.17[c]	0.41[c]	−0.8[c]

[a]All of these were conducted within 300 km of the surface site, and the 25 June, 26 June, 9 July and 17 July cases were conducted within 150 km of the surface site.
[b]Analysis of in-cloud data.
[c]Analysis of below-cloud data.

nally mounted PCASP, on the M-IV, and at the surface site. The inlet data obtained from the test flight show that PCASP concentrations increase by a factor of 2 when switching from the reverse-flow inlet to the isokinetic M-IV inlet. Of relevance to the CCN measurements made on the M-IV, it should be mentioned that these were acquired by sampling via an isokinetic inlet [*Snider and Brenguier*, 2000].

[61] 2. An analysis of measurements of the wet particle size spectra, at ambient humidity (87 to 97% RH), and their comparison to predicted wet size spectra show that the observed particle concentrations, in a relatively narrow size range (0.38 to 0.8 μm) are a factor of 2 to 10 smaller than those predicted. Surface HTDMA measurements show no evidence of a less-hygroscopic growth mode. Hence, the presence of particles not able to take up water, and thus incapable of growing to the sizes anticipated by our model, is not a viable explanation for the disparity. In contrast DMA sizing bias resulting from the incorrect assumption that mobility equivalent and spherical equivalent sizes are equal may also make a substantial contribution to the disparity. This issue is addressed further in part 2. Bias in the FSSP-300 measurement of either particle size or concentration cannot be discounted, but these are thought to be small relative to the discrepancies seen in Figures 9a, 9b, and 10. Finally limitations of the sampling procedure must be acknowledged. FSSP-300 samples were selected from below-cloud flight segments and criteria were used, in addition to the condition on the measured relative humidity, for rejecting data segments affected by droplets or drops. Further, if the criterion than the concentration of particles larger 3 μm is omitted, then the averaged spectra exhibit larger spectral densities at supermicron sizes but not in the size range that was the basis for comparing to the measurements made with the surface site DMA spectra. An important issue for the design of further experiments will be the improvement and intercomparison of measurement systems used to evaluate wet aerosol size spectra. This need is most acute at sizes smaller than 5 μm.

[62] In summary, CN and accumulation mode aerosol concentrations, and aerosol size spectra, measured by a variety of platforms during the CLOUDCOLUMN component of ACE-2 are consistent within experimental uncertainties. This result corroborates the assumption that the aerosol measurements made at the Punta del Hidalgo surface site are representative of aerosol entering clouds forming upwind of the surface site. This assumption is central to the closures studies performed in part 2. Also analyzed, and used as input data in part 2, are the airborne measurements of vertical velocity. Exceptions to our general conclusion are documented and users of the data set should heed those caveats. In addition it should be noted that

Table 2b. Vertical Velocity Statistics for the Flights Either Not Analyzed by *Pawlowska and Brenguier* [2000] or for the Cases That Were but Exhibited Spatially Nonuniform Distributions of CN and Accumulation Mode Aerosol Concentrations

Date	Flight Type	Cloud Base Altitude, m	Altitude of Sampling, m	Number of Data Points	Median Value, m/s	Average Value, m/s	Standard Deviation, m/s	Skewness
21 June	test	1397	1575[a]	1200[a]	0.26[a]	0.22[a]	0.45[a]	−0.2[a]
			512[b]	3000[b]	−0.35[b]	−0.34[b]	0.37[b]	−0.7[b]
24 June	test	1057	1125[a]	8732[a]	0.39[a]	0.36[a]	0.33[a]	−0.1[a]
			839[b]	2400[b]	0.36[b]	0.38[b]	0.30[b]	0.6[b]
4 July	SCI	800	1111[a]	2401[a]	0.24[a]	0.20[a]	0.50[a]	0.7[a]
7 July	SCI	600	700 and 768[a]	10,702[a]	0.13[a]	0.11[a]	0.43[a]	0.2[a]
			448 and 570[b]	12,000[b]	0.15[b]	0.14[b]	0.32[b]	0.2[b]
8 July	SCI*	707	715 and 785[a]	21,700[a]	0.13[a]	0.09[a]	0.45[a]	−1.0[a]
			500[b]	12,500[b]	0.12[b]	0.12[b]	0.45[b]	−0.3[b]
16 July	SCI*	883	990 and 1040[a]	10,800[a]	0.06[a]	0.03[a]	0.33[a]	−0.6[a]
			690 and 860[b]	17,000[b]	0.13[b]	0.11[b]	0.27[b]	−1.0[b]
19 July	SCI*	846	1000[a]	7191[a]	0.12[a]	0.08[a]	0.45[a]	0.0[a]
			470[b]	32,400[b]	0.00[b]	−0.04[b]	0.37[b]	−0.9[b]

[a]Analysis of in-cloud data.
[b]Analysis of below-cloud data.

aerosol mixing ratios were spatially nonuniform on 7, 16 and 19 July. Clearly these days must be excluded from analyses that synthesize both surface and airborne ACE-2 measurements.

[63] Beyond their use in part 2, these results will also be useful for constraining simulations of the CLOUDYCOLUMN cases and for the development and validation of model parameterizations. (The complete data set can be obtained by contacting J.-L. Brenguier at jlb@meteo.fr).

[64] **Acknowledgments.** We thank Terry Deshler for critiquing a draft of this manuscript. This work was supported by the European Union (grant EVK2-CT-1999-00054), by Météo-France and CNRS, and by the National Science Foundation (grants ATM-9816119 and ATM-0103951).

References

Albrecht, B. A., Aerosol, cloud microphysics, and fractional cloudiness, *Science*, *245*, 1227–1230, 1989.

Baumgardner, D., J. E. Dye, B. W. Gandrud, and R. G. Knollenberg, Interpretation of measurements made by forward scattering spectrometer probe (FSSP-300) during the Airborne Arctic Stratospheric Expedition, *J. Geophys. Res.*, *97*, 8035–8046, 1992.

Bigg, E. K., Discrepancy between observation and prediction of concentrations of cloud condensation nuclei, *Atmos. Res.*, *20*, 82–86, 1986.

Boers, R., J. B. Jensen, and P. B. Krummel, Microphysical and shirt-wave radiative structure of stratocumulus clouds over the Southern Ocean: Summer results and seasonal differences, *Q. J. R. Meteorol. Soc.*, *124*, 151–168, 1998.

Brenguier, J. L., T. Bourrianne, A. Coelho, J. Isbert, R. Peytavi, D. Trevarin, and P. Wechsler, Improvements of droplet size distribution measurements with the Fast-FSSP, *J. Atmos. Oceanic. Technol.*, *15*, 1077–1090, 1998.

Brenguier, J. L., H. Pawlowska, L. Schüller, R. Preusker, J. Fischer, and Y. Fouquart, Radiative properties of boundary layer clouds: Droplet effective radius versus number concentration, *J. Atmos. Sci.*, *57*, 803–821, 2000a.

Brenguier, J. L., Y. Chuang, Y. Fouquart, D. W. Johnson, F. Parol, H. Pawlowska, J. Pelon, L. Schüller, F. Schröder, and J. R. Snider, An overview of the ACE-2 CLOUDYCOLUMN Closure Experiment, *Tellus, Ser. B*, *52*, 814–826, 2000b.

Brown, E. N., Measurement uncertainties of the NCAR air motion system, *NCAR Tech. Note, NCAR/TN-386+STR*, 1993.

Chuang, P. Y., D. R. Collins, H. Pawlowska, J. R. Snider, H. H. Jonsson, J. L. Brenguier, R. C. Flagan, and J. H. Seinfeld, CCN measurements during ACE-2 and their relationship to cloud microphysical properties, *Tellus, Ser. B*, *52*, 842–866, 2000.

Collins, D. R., et al., In situ aerosol-size distributions and clear-column radiative closure during ACE-2, *Tellus, Ser. B*, *52*, 498–525, 2000.

Covert, D. S., J. L. Gras, A. Wiedensohler, and F. Stratmann, Comparison of directly measured CCN with CCN modeled from the number-size distribution in the marine boundary layer during ACE 1 at Cape Grim, Tasmania, *J. Geophys. Res.*, *103*, 16,597–16,608, 1998.

Ghan, S. J., C. Chuang, and J. E. Penner, A parameterization of cloud droplet nucleation, part I: Single aerosol type, *Atmos. Res.*, *30*, 197–222, 1993.

Guibert, S., Validation experimentale des parameterisations de l'effet indirect des aerosols, doctoral dissertation, Univ. Toulouse III-Paul Sabatier, France, 2002.

Johnson, D. W., et al., An overview of the Lagrangian Experiments undertaken during the North Atlantic Regional Aerosol Characterization Experiment (ACE-2), *Tellus, Ser. B*, *52*, 290–320, 2000.

Martinsson, B. G., et al., Validation of very high cloud droplet number concentrations in air masses transported during thousands of kilometers over the ocean, *Tellus, Ser. B*, *52*, 801–814, 2000.

Neusüß, C., D. Weise, W. Birmili, H. Wex, A. Wiedensohler, and D. S. Covert, Size-segregated chemical, gravimetric and number distribution-derived mass closure of the aerosol in Sagres, Portugal during ACE-2, *Tellus, Ser. B*, *52*, 169–184, 2000.

Panofsky, H. A., and J. A. Dutton, *Atmospheric Turbulence*, John Wiley, Hoboken, N. J., 1984.

Pawlowska, H., and J. L. Brenguier, Microphysical properties of stratocumulus clouds during ACE-2, *Tellus, Ser. B*, *52*, 867–886, 2000.

Petzold, A., et al., Near-field measurements on contrail properties from fuels with different sulfur content, *J. Geophys. Res.*, *102*, 29,867–29,880, 1997.

Putaud, J. P., R. Van Dingenen, M. Mangoni, A. Virkkula, H. Maring, J. M. Prospero, E. Swietlicki, O. H. Berg, R. Hillamo, and T. Mäkelä, Chemical mass closure and assessment of the origin of the submicron aerosol in the marine boundary layer and the free troposphere at Tenerife during ACE-2, *Tellus, Ser. B*, *52*, 141–168, 2000.

Quinn, P. K., D. S. Covert, T. S. Bates, V. N. Kapustin, D. C. Ramsay-Bell, and L. M. McInnes, Dimethylsulfide/cloud condensation nuclei/climate system: Relevant size-resolved measurements of the chemical and physical properties of atmospheric aerosol particles, *J. Geophys. Res.*, *98*, 10,411–10,427, 1993.

Quinn, P. K., T. S. Bates, D. J. Coffman, T. L. Miller, J. E. Johnson, D. S. Covert, J.-P. Putaud, C. Neusüß, and T. Novakov, A comparison of aerosol chemical and optical properties from the 1st and 2nd Aerosol Characterization Experiments, *Tellus, Ser. B*, *52*, 239–257, 2000.

Raes, F., T. Bates, F. McGovern, and M. Van Liedekerke, The second aerosol characterization experiment (ACE-2), General overview, and main results, *Tellus, Ser. B.*, *52*, 827–841, 2000.

Roode, S. R., and P. G. Duynkerke, Dynamics of cumulus rising into stratocumulus as observed during the first 'Lagrangian' experiment of ASTEX, *Q. J. R. Meteorol. Soc.*, *122*, 1597–1623, 1996.

Schröder, F., and J. Ström, Aircraft measurements of sub micrometer aerosol particles (>7 nm) in the midaltitude free troposphere and tropopause region, *Atmos. Res.*, *44*, 333–356, 1997.

Sioutas, C., E. Abt, J. M. Wolfson, and P. Koutrakis, Evaluation of the measurement performance of the scanning mobility particle sizer and aerodynamic particle sizer, *Aerosol Sci. Technol.*, *30*, 84–92, 1999.

Snider, J. R., and J. L. Brenguier, Cloud condensation nuclei and cloud droplet measurements during ACE-2, *Tellus, Ser. B*, *52*, 827–841, 2000.

Snider, J. R., S. Guibert, J.-L. Brenguier, and J.-P. Putaud, Aerosol activation in marine stratocumulus clouds: 2. Köhler and parcel theory closure studies, *J. Geophys. Res.*, *108*(D15), 8629, doi:10.1029/2002JD002692, in press, 2003.

Swietlicki, E., et al., Hygroscopic properties of aerosol particles in the north-eastern Atlantic during ACE-2, *Tellus, Ser. B*, *52*, 201–227, 2000.

Twomey, S., The influence of pollution on the shortwave albedo of clouds, *J. Atmos. Sci.*, *34*, 1149–1152, 1977.

Van Dingenen, R., A. O. Virkkula, R. F. Raes, T. S. Bates, and A. Wiedensohler, A simple non-linear analytical relationship between aerosol accumulation number and sub-micron volume, explaining their observed ratio in the clean and polluted marine boundary layer, *Tellus, Ser. B*, *52*, 452–561, 2000.

VanZanten, M. C., P. G. Duynkerke, and J. W. M. Cuijpers, Entrainment parameterization in convective boundary layers derived from large eddy simulations, *J. Atmos. Sci.*, *56*, 813–828, 1999.

Verver, G. E., F. Raes, D. Vogelezang, and D. Johnson, The 2nd Aerosol Characterization Experiment (ACE-2), Meteorological and chemical context, *Tellus, Ser. B*, *52*, 127–140, 2000.

Wood, R., et al., Boundary layer and aerosol evolution during the third Lagrangian experiment of ACE-2, *Tellus, Ser. B*, *52*, 401–422, 2000.

J.-L. Brenguier and S. Guibert, Centre National de Recherche Météorologique (CNRM), GMEI/D, Météo-France, F-31057 Toulouse Cedex 01, France. (jlb@meteo.fr; guibert@cnrm.meteo.fr)

J. R. Snider, Department of Atmospheric Science, University of Wyoming, Laramie, WY 82701, USA. (jsnider@uwyo.edu)